MATERIALS CHEMISTRY
FRONTIERS

RESEARCH ARTICLE

View Article Online
View Journal

Cite this: DOI: 10.1039/d4qm00714j

Elementary processes in ternary solar cells†

Teodoro Pizza, [ab] Alessandro Landi, *[a] Francesco Ambrosio, [c] Amedeo Capobianco *[a] and Andrea Peluso [a]

The insertion of a third component in bulk heterojunction solar cells has led to enhanced power conversion efficiencies (PCEs). However, the rationale beyond the superior performance of ternary solar cells (TSCs) is still a matter of debate and device design is usually based on qualitative considerations. Herein, we present an exhaustive analysis of the kinetics of interfacial charge and energy transfer elementary processes occurring in an archetypal ternary blend, composed of two donors (FG3 and FG4) and one acceptor (Y6). Using molecular dynamics (MD) simulations to generate realistic blend morphologies, coupled with a full quantum mechanical approach to compute reaction rates, we provide insights into the factors contributing to the final PCE of TSCs. Our results indicate that, for the system under study, the presence of two donors allows for more effective solar spectrum coverage, while Förster resonance energy transfer plays a key role in funneling the energy absorbed by FG3 towards a more kinetically efficient FG4:Y6 donor–acceptor pair. Indeed, the FG3:Y6 combination is hampered by slower charge transfer rates, primarily due to energy loss pathways. These findings indicate that even small differences between donor molecules (such as FG3 and FG4) can lead to dramatically different charge transfer kinetics, suggesting that the improved PCE observed in TSCs cannot be easily anticipated through qualitative assessments alone. Instead, device performance is highly sensitive to the intricate interplay of charge and energy transfer processes, highlighting the need for theoretical modeling to accurately predict outcomes. In this respect, we show that our protocol can provide useful elements for a deeper understanding of the physical effects concurring to determine the final PCE of a device, thus enabling a rational design of novel blends for organic solar cells.

Received 19th August 2024,
Accepted 30th September 2024

DOI: 10.1039/d4qm00714j

rsc.li/frontiers-materials

Organic solar cells (OSCs) have been the focus of intense research activity during the last few decades,[1–7] in light of their potential advantages over traditional silicon-based devices,[8] namely cheap fabrication processes and chemically tunable electronic and optical properties.[8–13]

The active layer of an OSC is typically constituted by two main components: an electron donor (D) and an electron acceptor (A), whose energy levels need to be properly aligned not only for maximizing charge transfer across their interface but, probably more importantly, also for minimizing charge recombination.[5,7,14] The most popular architecture for OSCs is the bulk heterojunction (BHJ), in which A and D domains are intermixed,[15] thus ensuring a hetero-interface distributed throughout the whole bulk of the active layer and the required film thickness for adequate absorption of radiation, while reducing the distance to travel for excitons to reach the A/D interface. Notwithstanding the appreciable improvements that have been achieved in the last few years,[16–19] significant issues still need to be overcome, in order to make BHJ solar cells a viable technology for the future. In fact, while the substitution of traditional A molecules, based on fullerenes, with more efficient molecular semiconductors (*e.g.* Y6 and its derivatives)[17,20] has led to power conversion efficiencies (PCEs) larger than 19%,[16–19] not only these efficiencies are far from the theoretical Shockley–Queisser limit of 33% for single junction devices,[21] but the performance gap with traditional and perovskite-based inorganic solar cells (PCE > 25%[22,23]) is still substantial.[24]

Over the past decade, numerous strategies have been proposed to improve the PCE of single-junction devices.[25–27] Among them, the introduction of a third component into the BHJ active layer, thus effectively constructing a ternary solar cell (TSC), has rapidly attracted interest.[28,29] In fact, if thoroughly

[a] *Dipartimento di Chimica e Biologia, Università di Salerno, Via Giovanni Paolo II, Fisciano, Salerno I-84084, Italy. E-mail: alelandi1@unisa.it, acapobianco@unisa.it*
[b] *Dipartimento di Chimica, Biologia e Biotecnologie, Università degli Studi di Perugia, Via Elce di Sotto, 8, Perugia (PG) I-06123, Italy*
[c] *Dipartimento di Scienze, Università degli Studi della Basilicata, Viale dell'Ateneo Lucano, Potenza (PZ) 10 I-85100, Italy*

† Electronic supplementary information (ESI) available: Details about FGR and MD calculations, computational details, FCWDs for all processes, prototypical configurations of the molecules extracted from MD, molecular orbitals for some of these configurations, and the kinetic model used for the binary cell. See DOI: https://doi.org/10.1039/d4qm00714j

chosen, a third component may lead to higher efficiencies even when added to otherwise poor binary devices. Probably, the main reason is that a third component can enhance the performances of binary devices both from an electronic and a morphological point of view. From the electronic point of view, it has been suggested that the inclusion of a third component can boost photon energy harvesting and provide panchromatic absorption. This, in turn, may lead to the enhancement of the short-circuit current (J_{SC}), open-circuit voltage (V_{OC}) and fill factor (FF) of the cell, with respect to binary devices.[29] Higher efficiencies have also been ascribed to new charge and energy transfer channels opening in the blend.[28] From the morphological point of view, crystallinity may be enhanced, at the price of having a more complicated morphology control with respect to binary devices.[29] Nevertheless, TSCs can maintain the single-step layer processing fabrication typical of single-junction OSCs. To date, TSCs with efficiency higher than 19% have been reported,[30–33] giving strong confidence toward reaching efficiencies seen in inorganic devices in the near future.

These higher efficiencies are achieved because the ternary component can modulate both the morphology and the energetics of the photophysical processes occurring in the device; moreover, new charge and energy transfer mechanisms are introduced into the blend thanks to the new component.[34] In this regard, four main working mechanisms have been proposed in the literature, unique to TSCs, that could explain the better performances of these devices with respect to their binary counterparts:[28] (i) energy transfer between "host" and "guest" donors (acceptors); (ii) charge transfer between "host" and "guest" donors (acceptors); (iii) charge transfer between the "host" and the "guest" donors (acceptors) and the "host" acceptor (donor), where the two donors (acceptors) act separately like in a tandem device; (iv) charge transfer between an alloy composed of the "host" and "guest" donors (acceptors) and the "host" acceptor (donor). Each one is related to a specific ternary blend morphology, but usually more than one mechanism is at work for charge and energy transfer processes in the same cell,[28,35] making experimental and theoretical studies extremely challenging. Indeed, a comprehensive understanding of the factors actually contributing to the enhanced efficiencies of TSCs has not been achieved yet.[28,29]

Let us consider, for example, the archetypal ternary blend made by two D molecules, FG3 and FG4, and the non-fullerene A, Y6, *cf.* Fig. 1(a). These molecules, featuring extended π delocalization, possess similar electrochemical energy gaps in the visible region of the spectrum (*cf.* ref. 36 and 37 and ESI†). Power conversion efficiencies greater than 14% have been reported for FG3:FG4:Y6,[36] to be compared with the less performing FG3:Y6 (10.75%) and FG4:Y6 (11.07%) binary cells. We note that, with respect to polymer ones, small-molecule systems (such as the one under study) usually display higher batch-to-batch replicability,[38] and therefore, can serve as reliable reference models.

The roughly 30% relative increase in PCE for the TSC may be in principle ascribed to the broader absorption of the blend. This can be quantitatively assessed by evaluating the so-called useful fraction (UF),[39,40] *i.e.* the relative overlap of the experimental spectral responses of the blend, S_R and the solar spectral irradiance S_I at the sea level (AM1.5, AM being the air mass coefficient),[41] which is connected with the device's short circuit current per area (I_{SC}/A), and therefore with the PCE.[42] In Fig. 1(b), we report the AM1.5 spectrum and the experimental spectral responses[36] for the TSC and the binary OSCs under study. It is evident that FG4:Y6 possesses a spectral response spanning a smaller wavelength range than that of FG3:Y6 and FG3:FG4:Y6, and that it has a reduced overlap with the solar spectrum. Indeed, our calculated values of UF are 37%, 40% and 43% for FG4:Y6, FG3:Y6 and the ternary cell, respectively. However, these values do not directly correlate with measured PCEs: while the TSC is indeed more efficient than the binary cells, the FG4:Y6 and FG3:Y6 blends show very similar PCE values, with the former being even better, notwithstanding a 3% gap in the estimated UFs. This suggests that TSC architectures cannot be designed solely on the basis of spectral properties and aiming only at panchromatic absorption may not be the optimal strategy for rationale material design.

Therefore, an in-depth study of the energy and charge transfer processes occurring in the ternary blend is truly necessary.[14,43] However, these are rarely accessible from the experiment; besides, usually more than one mechanism is operative in the same cell[28,29,35] and disentangling the different effects makes theoretical studies extremely challenging. In this context, it has been suggested that the Förster resonant energy transfer (FRET) mechanism between the S_1 states of the two donors may play a key role.[36,44] The calculated $S_1 \rightarrow S_0$ Franck–Condon weighted density of states (FCWD) of FG3 and the $S_1 \leftarrow S_0$ FCWD of FG4 (*cf.* ESI† for computational details) seem to confirm such a hypothesis:[36] in fact, the two computed spectral distributions overlap to a large extent and the S_1 level of FG3 lies 0.26 eV above that of FG4. This suggests that FRET from FG3 to FG4 is very likely to happen at the interface, further confirming the results obtained by Guijarro *et al.* (ref. 36). Therefore, it should be included as an extra energy transfer pathway, in addition to those usually accounted for in a binary OSC, *cf.* Fig. 1(d), *i.e.* (i) the formation of a charge transfer (CT) state *via* either photoinduced electron transfer from the S_1 state of the D molecule (here either PET_{FG3} or PET_{FG4}) or (ii) *via* photoinduced hole transfer from the S_1 state of A (PHT_{Y6}), (iii) D–A excitation energy transfer (EET_{FG3}, EET_{FG4}) and (iv) charge recombination (CR). The Jablonski diagram for the three components of the ternary blend, *cf.* Fig. 1(e), shows that both PET_{FG3} and PET_{FG4} are feasible, since the first excited singlet state of both FG3 and FG4 are higher in energy than the corresponding charge transfer (CT) states. Also PHT_{Y6} is energetically allowed, indicating that several dissociation channels could be in competition with each other. Fig. 1 also shows that FRET between the S_1 states of the two donors has to be considered, ultimately leading to the CT state through PET_{FG4}.

The final efficiency of the solar cell will certainly depend on the relative rates of these interfacial charge and energy transfer processes;[43,45] those rates can be estimated using Fermi's golden rule (FGR), provided that its limits of applicability are met. According to such a full quantum mechanical approach, the non radiative transition rate between two electronic states

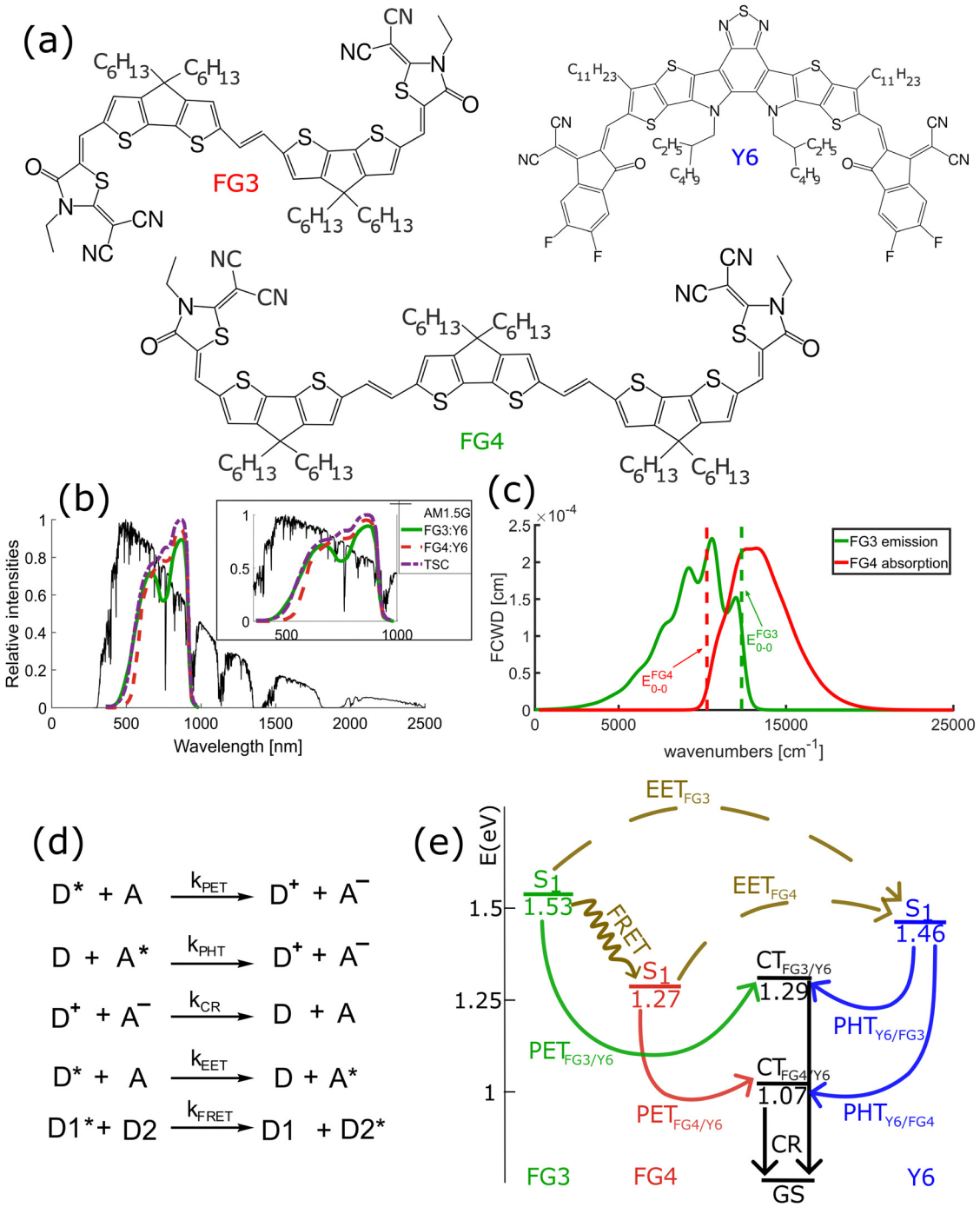

Fig. 1 (a) Chemical structures of the molecules studied in this work. (b) Spectral response (from ref. 36) and solar irradiation AM1.5. The inset shows a zoomed-in view of the wavelength range spanned by the spectral responses. (c) Predicted FCWD for $S_1 \rightarrow S_0$ emission of FG3 (full green line) and for $S_1 \leftarrow S_0$ absorption of FG4 (dashed red line). E_{0-0} energies for $S_1 \leftarrow S_0$ absorption energies are indicated as vertical dotted lines. (d) Scheme of possible charge and energy transfer processes occurring at the $D_1/D_2/A$ interface. D without subscript may refer to both D_1 and D_2. The ΔE of these reactions can be found in the ESI.† (e) Jablonski diagram of the ternary blend.

$|i\rangle$ and $|f\rangle$, with an electronic energy difference ΔE_{if}, is:

$$k_{if} = \frac{2\pi}{\hbar}|J_{if}|^2 F(\Delta E_{if}, T) \quad (1)$$

where J_{if} is the electronic coupling element between initial and final states, *i.e.* the interaction strength, and $F(\Delta E_{if},T)$ is the Franck–Condon weighted density of states (FCWD):

$$F(\Delta E_{if}, T) = \sum_{\nu_f,\nu_i} |\langle \nu_f|\nu_i\rangle|^2 e^{-\beta E_{\nu_i}} \delta\left(E_{\nu_f} - E_{\nu_i} + \Delta E_{if}\right)/Z_i, \quad (2)$$

where T is the temperature, $\beta = 1/(k_B T)$, with k_B as the Boltzmann constant, E_{ν_j} the vibrational energy of the j-th electronic

states, Z_i the vibrational partition function of the initial state, and $\langle v_f|v_i\rangle$ the Franck–Condon integral. $F(\Delta E_{if},T)$ accounts for the effect of nuclear configuration changes accompanying the electronic transition, evaluated at ΔE_{if}, the electronic energy difference of the transition (*cf.* Section S1.3 and Table S3 in the ESI†). This approach has proven to yield extremely reliable rates for both radiative and non-radiative processes.[46–51] FCWDs are here computed *via* the generating function approach[52–54] in conjunction with the harmonic approximation for molecular vibrations. The latter are evaluated through electronic structure calculations on the isolated molecules (*cf.* ESI† and ref. 50 and 55), as small intermolecular interactions are not expected to significantly affect them.

At variance with this, the estimation of the electronic coupling terms appearing in eqn (2) requires the attainment of a realistic description of the blend morphology, as this quantity is decidedly affected by the relative position of the interacting molecules. Therefore, we have here performed classical molecular dynamics simulations (see Section S1.2 of the ESI† for further details), which are known to lead to molecular packings in good agreement with the experiment,[56] thus providing reliable models for the investigation of the underlying optoelectronic properties.[56,57] We consider the experimental ratio of components (D : A = 0.40 : 0.60 in binary devices, and FG3 : FG4 : Y6 = 0.12 : 0.28 : 0.60 in the ternary one),[36] *cf.* Fig. 2(a) and ESI† for computational details. 100 geometries equispaced in time (available at the following public GitHub repository: **https://github.com/XelaleX1/TSC_paper**) for each couple FG3/Y6, FG4/Y6 (and FG3/FG4 for the ternary cell) are extracted from the last 40 ns of MD trajectories for both binary and ternary model systems (*cf.* Fig. 2(b) for representative structural configurations).

For each of these snapshots, we compute the electronic couplings for all the relevant processes. In particular, for PHT, PET and CR processes, the electronic couplings are calculated as $J_{ij} = \langle \phi_i|\hat{F}|\phi_j\rangle$, where ϕ_i and ϕ_j are the unperturbed frontier orbitals of the isolated D and A, respectively, and $\hat{F}$ is

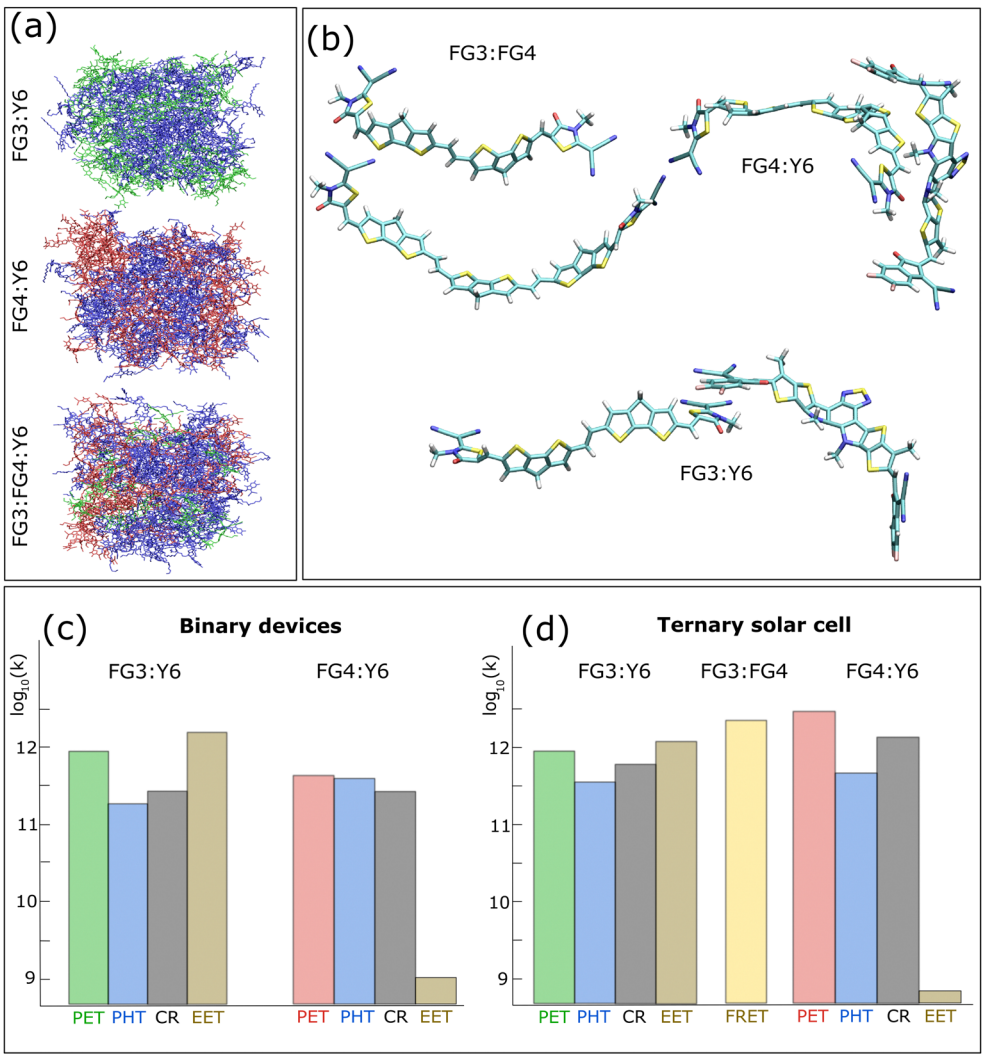

Fig. 2 (a) Pictorial representation of the final topology in MD simulations. (b) Representative structural configurations having high electronic coupling for pairs extracted from MD simulations of the ternary blend (C in cyan, H in white, N in blue, O in red and S in yellow). Average rates for all the studied energy and charge transfer processes for (c) the binary FG3:Y6 and FG4:Y6 blends and (d) the FG3:FG4:Y6 ternary system.

the Kohn–Sham–Fock operator of the D/A pair.[58–60] Instead, FRET and EET couplings are evaluated by resorting to a perturbative approach from the transition densities of the non-interacting units,[43,61,62] as implemented in the Gaussian16 package.[63] Supplementary details on the performed calculations and average calculated values of J for each process in both binary and ternary blend models are given in Section S1.2 of the ESI.†

All the calculated average rates for binary and ternary cells are reported in Fig. 2(c) and (d). We first focus on the binary FG3:Y6 and FG4:Y6 devices. For the FG4:Y6 blend, the PET rate is of the order of a few ps^{-1}, as expected from transient absorption spectra of a generic organic photovoltaic blend.[64] PHT and CR rates are of the same order of magnitude as the PET one, while EET_{FG4} is predicted to be much slower (ns^{-1}), being energetically slightly disfavoured (ΔE = +0.19 eV), so that EET plays a very marginal role in this blend, see also the results below. The FG3:Y6 blend shows striking differences compared to FG4:Y6. Indeed in FG3:Y6, EET_{FG3} is the fastest process, being slightly exergonic (ΔE = −0.07 eV) (*cf.* Section S1.3 in the ESI†). Furthermore, EET_{FG3} is even faster than PET_{FG3}, thus suggesting that the energy transfer distinctly competes with the dissociation of the S_1 state of the donor into CT. This, together with the low rate for PHT_{Y6} (*ca.* one order of magnitude lower than that of PET_{FG3}), indicates that the formation of the CT state could be less favoured for FG3:Y6 than for FG4:Y6.

In order to better appreciate this point, the Pauli master equation approach has been used to study the irreversible dynamics at the A/D interface in terms of populations over time of the different electronic states involved in the energy and charge transfer elementary processes, (see Section S3 in the ESI† for more details).[43,65] In Fig. 3, we depict the time-dependent evolution of the populations of the electronic states, for an initial condition corresponding to a local excitation of the donor (P_{D^*} = 1). From panel (a) of Fig. 3 it is clear that, at the beginning, the CT intermediate coexists with the local excitation on the acceptor Y6*, which is the dominant species for a larger time interval. In fact, EET_{FG3} being faster than PET_{FG3} and, the formation of CT state from Y6* (PHT_{FG3}) being comparatively slower than PET_{FG3}, a higher population of Y6* is obtained rather than the CT state in the FG3:Y6 device. Indeed, the CT state is the predominant species only in a very small time interval (less than 1 ps). On the other hand, from panel (b) of Fig. 3 it is clear that the only populated intermediate is the CT state, having (i) a higher maximum population than for FG3:Y6 blend, and most importantly (ii) being the predominant species for a larger time interval. This is easily rationalized on the basis of the extremely slow EET_{FG4}, and the fast PET_{FG4}, so that the excited donor quickly interconverts into the CT state. Those results indicate that while the FG3:Y6 blend features a better spectral response, such an advantage over the FG4:Y6 system is completely lost, as a consequence of poorer charge transfer kinetics. In fact, we can rationalize the similar measured PCE values for FG3:Y6 and FG3:Y4 (10.75% *vs.* 11.07%[36]) in terms of the competition between spectral response (favouring FG3) and ease of exciton dissociation (faster in FG4).

Incidently, we notice that the kinetic processes shown in Fig. 3 occur on a timescale similar to that of the mutual local fluctuations of the molecules involved.[66] However, this does not affect our predictions, since local fluctuations are already accounted for in our model. Indeed all the normal modes of the interacting molecules are included in our FGR approach, while slower molecular motions are considered in our protocol by averaging the rates of photophysical processes over a distribution of molecular conformations sampled from the MD trajectory, as discussed above.

Finally, we discuss the ternary system: from Fig. 2(c), we note that rates of the processes occurring at the FG3/Y6 interface in the TSC broadly resemble those observed for the binary system. In stark contrast, both PET and CR for FG4/Y6 are predicted to be faster by almost one order of magnitude in the TSC. This effect, connected with the increase of the electronic couplings between FG4 and Y6, indicates that more favourable interactions are established between FG4 and Y6 in the ternary cell, as compared to the binary device. Such a result corroborates the experimental assumption, based on X-ray measurements, that a more compact structure in the ternary cell may

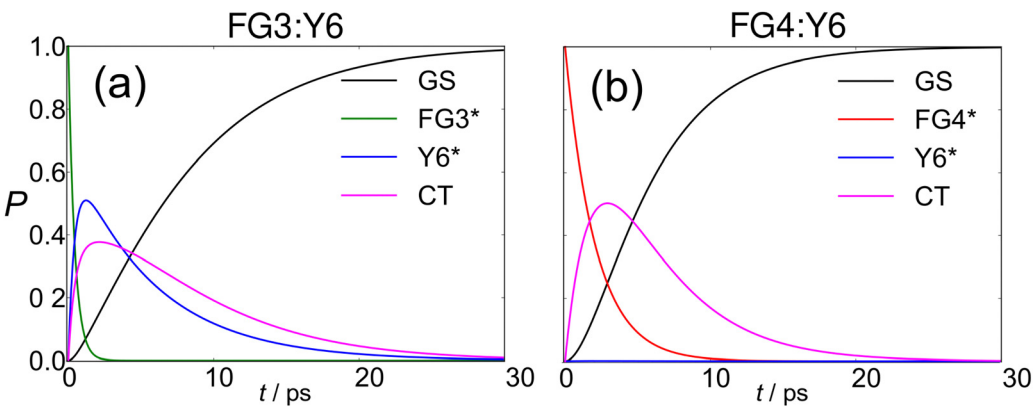

Fig. 3 Time-dependent evolution of state populations for FG3:Y6 (a) and FG4:Y6 (b). We consider an initial condition corresponding to a local excitation of the donor (P_{D^*} = 1). The labels GS, X* and CT refer, respectively, to the ground state, a local excitation on the molecule X, and the charge transfer state, *cf.* ESI.†

augment the π–π stacking in the TSC,[36] but with the caveat, here evidenced, that this in turn also amplifies recombination.

We have also investigated the possible involvement of a cascade hole transfer mechanism, forming a CT state with reduced binding energy, for instance $FG4^{+}$:FG3:$Y6^{-}$, which could reduce CR rates and enhance charge dissociation rates, as it occurs in the early electron transfer steps in photosynthetic reaction centers. We have thus extracted snapshots from MD simulations of the ternary cell, where FG3 was placed in a bridge position between FG4 and Y6. However, none of the extracted configurations proved to be very effective: configurations with lower charge recombination rates were all characterized by low rates of PET and PHT processes. We have also investigated the possible involvement of triplet states in these blends, which could provide CT states with longer lifetimes,[34,45,67] thus aiding the formation of free charges. However, it has been pointed out in the literature[68,69] that while the impact of triplet states in solar cells based on fullerene acceptors is substantial, it is expected to be minor in devices based on non-fullerene acceptors, in particular fluorinated ones,[68] such as the Y6 considered here. Moreover, for the blends under study in our work, the unfavourable energy differences and the small spin–orbit coupling (see the ESI†) elements also prevent the possible involvement of triplet states in this specific system, so the key factor for the superior performance of this ternary solar cell is represented by the FRET between the two donors.[36]

In conclusion, here we have presented a combination of MD and FGR simulations for the description of elementary energy and charge transfer processes in ternary solar cells. The reliability of this protocol has been extensively proven in the past by some of us in the field of binary solar cells[14,43] and more in general on various organic semiconductors.[70] In this work, we focused our attention on a prototypical system, formed by FG3:FG4:Y6, to be used as proof-of-principle for the extension of our protocol to ternary devices; the natural extension of this work resides in studying a larger number of systems, and work is ongoing in our group along that line. This preliminary study has allowed relating the higher PCE of the TSC to the integration of at least two factors: (i) the presence of two donors, which allows exploiting a wider region of the solar spectrum and (ii) a favourable FRET, which conveys all the energy absorbed by FG3 towards the kinetically more efficient FG4:Y6 couple. The lower performances of the FG3:Y6 pair are mainly due to the fact that the depopulation of FG3* is found to take place not only *via* PET but also *via* EET towards Y6*, whose slower PHT remains the weak link in the chain. Therefore, our in-depth analysis indicates that the extent in PCE raise attainable *via* a TSC strategy cannot be easily predicted by qualitative considerations, which, contrarily, may actually hinder the progress in the field.

In fact, we have seen here (when comparing FG4:Y6 with FG3:Y6) that any gain achieved by extending the spectral range *via* panchromatic absorption might be lost to unfavourable charge and energy transfer kinetics and that even strengthening of intermolecular interaction can be a double-edged sword, as it can speed up both charge separation and decay channels (as occurred here when passing from FG4:Y6 to the TSC device). Thus, it is fundamental to underline that, when conceiving novel blends, the full landscape of the operative processes cannot be portrayed a priori, without the help of appropriate theoretical modelling, as it strongly depends upon the microscopic nature of intermolecular interactions. For example, we here observe that two very similar molecules, FG3 and FG4, can display extremely different charge transfer kinetics in the device and that the rationalization of measured PCEs defies simplistic interpretations. From another point of view, this also indicates that the main mechanism responsible of the efficiency enhancement in a ternary solar cell is system-dependent, to the point that even if FRET is widely explored to take advantage of complementary absorption and bandgap tuning,[34] it does not always improve the performance of the blend: in some cases the introduction of a third component worsens the photoconversion efficiency, *e.g.* because of a reduced energy offset between the guest donor and the acceptor.[34,71]

In this context, computational modelling can verily provide a physically sound rationale to the PCE trends in binary and ternary cells, by accurately estimating the interplay between different processes occurring in the device, whose experimental assessment is generally beyond reach, due to the complexity of the device. Moreover, in light of its computational rapidity, the protocol presented here represents a powerful and reliable tool for predicting the performance of a wide range of organic materials, to identify the most promising systems for the fabrication of highly efficient organic solar cells.

Data availability

The data supporting this article have been included as part of the ESI† and at this public GitHub repository **https://github.com/XelaleX1/TSC_paper**.

Conflicts of interest

There are no conflicts to declare.

Acknowledgements

The financial support from Università degli Studi di Salerno is gratefully acknowledged. A. L. gratefully acknowledges the funding from the Italian Ministry of University and Research (MUR, PRIN grant 2022XSC9P5). A. L. acknowledges the CINECA award HP10CVHRXV (LIMES) under the ISCRA initiative, for the availability of high-performance computing resources and support. A. C. gratefully acknowledges the support funding from the Italian Ministry of University and Research (MUR, PRIN grant 2022KHEZTC). A. P. gratefully acknowledges the funding from the Italian Ministry of University and Research (MUR, PRIN grant 2022WXPMB).

References

1 Y. Wang, J. Lee, X. Hou, C. Labanti, J. Yan, E. Mazzolini, A. Parhar, J. Nelson, J.-S. Kim and Z. Li, *Adv. Energy Mater.*, 2021, **11**, 2003002.

2 J. Grüne, G. Londi, A. J. Gillett, B. Stähly, S. Lulei, M. Kotova, Y. Olivier, V. Dyakonov and A. Sperlich, *Adv. Funct. Mater.*, 2023, **33**, 2212640.

3 Y. Wang, J. Luke, A. Privitera, N. Rolland, C. Labanti, G. Londi, V. Lemaur, D. T. Toolan, A. J. Sneyd, S. Jeong, D. Qian, Y. Olivier, L. Sorace, J.-S. Kim, D. Beljonne, Z. Li and A. J. Gillett, *Joule*, 2023, **7**, 810–829.

4 S. H. Park, A. Roy, S. Beaupré, S. Cho, N. Coates, J. S. Moon, D. Moses, M. Leclerc, K. Lee and A. J. Heeger, *Nat. Photonics*, 2009, **3**, 297–302.

5 J. Benduhn, K. Tvingstedt, F. Piersimoni, S. Ullbrich, Y. Fan, M. Tropiano, K. A. McGarry, O. Zeika, M. K. Riede, C. J. Douglas, S. Barlow, S. R. Marder, D. Neher, D. Spoltore and K. Vandewal, *Nat. Energy*, 2017, **2**, 17053.

6 Z.-W. Zhao, O. H. Omar, D. Padula, Y. Geng and A. Troisi, *J. Phys. Chem. Lett.*, 2021, **12**, 5009–5015.

7 M. Azzouzi, J. Yan, T. Kirchartz, K. Liu, J. Wang, H. Wu and J. Nelson, *Phys. Rev. X*, 2018, **8**, 031055.

8 G. J. Hedley, A. Ruseckas and I. D. W. Samuel, *Chem. Rev.*, 2017, **117**, 796–837.

9 A. Köhler and H. Bässler, *Electronic Processes in Organic Semiconductors: An Introduction*, Wiley-VCH Verlag GmbH & Co. KGaA, 2015.

10 A. Landi, A. Peluso and A. Troisi, *Adv. Mater.*, 2021, **33**, 2008049.

11 J. Sun, X. Ma, Z. Zhang, J. Yu, J. Zhou, X. Yin, L. Yang, R. Geng, R. Zhu, F. Zhang and W. Tang, *Adv. Mater.*, 2018, **30**, 1707150.

12 A. Landi, M. Reisjalali, J. D. Elliott, M. Matta, P. Carbone and A. Troisi, *J. Mater. Chem. C*, 2023, **11**, 8062–8073.

13 N. Yeh and P. Yeh, *Renewable Sustainable Energy Rev.*, 2013, 421–431.

14 A. Landi, D. Padula and A. Peluso, *ACS Appl. Energy Mater.*, 2024, **7**, 707–714.

15 N. Yeh and P. Yeh, *Renewable Sustainable Energy Rev.*, 2013, **21**, 421–431.

16 J. Chen, J. Cao, L. Liu, L. Xie, H. Zhou, J. Zhang, K. Zhang, M. Xiao and F. Huang, *Adv. Funct. Mater.*, 2022, **32**, 2200629.

17 C. Li, J. Zhou, J. Song, J. Xu, H. Zhang, X. Zhang, J. Guo, L. Zhu, D. Wei, G. Han, J. Min, Y. Zhang, Z. Xie, Y. Yi, H. Yan, F. Gao, F. Liu and Y. Sun, *Nat. Energy*, 2021, **6**, 605–613.

18 M. Li, H. Lin, B. Ma, X. Yu, X. Du, G. Yang, C. Zheng and S. Tao, *J. Mater. Chem. C*, 2022, **10**, 3207–3216.

19 Y. Gao, X. Yang, W. Wang, R. Sun, J. Cui, Y. Fu, K. Li, M. Zhang, C. Liu, H. Zhu, X. Lu and J. Min, *Adv. Mater.*, 2023, **35**, 2300531.

20 L. Feng, J. Yuan, Z. Zhang, H. Peng, Z.-G. Zhang, S. Xu, Y. Liu, Y. Li and Y. Zou, *ACS Appl. Mater. Interfaces*, 2017, **9**, 31985–31992.

21 W. Shockley and H. J. Queisser, *J. Appl. Phys.*, 1961, **32**, 510–519.

22 K. Yoshikawa, H. Kawasaki, W. Yoshida, T. Irie, K. Konishi, K. Nakano, T. Uto, D. Adachi, M. Kanematsu, H. Uzu and K. Yamamoto, *Nat. Energy*, 2017, **2**, 17032.

23 B. M. Kayes, H. Nie, R. Twist, S. G. Spruytte, F. Reinhardt, I. C. Kizilyalli and G. S. Higashi, 2011 37th IEEE Photovoltaic Specialists Conference, 2011, 000004-000008.

24 M. A. Green, E. D. Dunlop, G. Siefer, M. Yoshita, N. Kopidakis, K. Bothe and X. Hao, *Prog. Photovoltaics*, 2023, **31**, 3–16.

25 Y. Tamai, *Adv. Energy Sustainability Res.*, 2023, **4**, 2200149.

26 M. Li and F. He, *Next Energy*, 2024, **2**, 100085.

27 B. Mohamed El Amine, Y. Zhou, H. Li, Q. Wang, J. Xi and C. Zhao, *Energies*, 2023, **16**, 3895.

28 Y. Zhang and G. Li, *Acc. Mater. Res.*, 2020, **1**, 158–171.

29 N. Gasparini, A. Salleo, I. McCulloch and D. Baran, *Nat. Rev. Mater.*, 2019, **4**, 229–242.

30 Z. Ling, M. I. Nugraha, W. T. Hadmojo, Y. Lin, S. Y. Jeong, E. Yengel, H. Faber, H. Tang, F. Laquai, A.-H. Emwas, X. Chang, T. Maksudov, M. Gedda, H. Y. Woo, I. McCulloch, M. Heeney, L. Tsetseris and T. D. Anthopoulos, *ACS Energy Lett.*, 2023, **8**, 4104–4112.

31 M. Peng, H. Wu, L. Wu, J. Chen, R. Ma, Q. Fan, H. Tan, W. Zhu, H. Li and J. Ding, *J. Energy Chem.*, 2024, **95**, 263–270.

32 G. Zhang, Q. Wu, Y. Duan, W. Liu, M. Zou, H. Zhou, J. Cao, R. Li, X. Xu, L. Yu and Q. Peng, *Chem. Eng. J.*, 2023, **476**, 146538.

33 C. Zhang, M. Lin, Y. Wei, R. Xu, Z. Zhang, X. Sun, H. Wang, H. Hu and K. Wang, *J. Mater. Chem. A*, 2024, **12**, 16502–16510.

34 T. Zhang and N. Gasparini, *Appl. Phys. Lett.*, 2022, **120**, 250501.

35 Y. M. Yang, W. Chen, L. Dou, W.-H. Chang, H.-S. Duan, B. Bob, G. Li and Y. Yang, *Nat. Photonics*, 2015, **9**, 190–198.

36 F. G. Guijarro, R. Caballero, P. de la Cruz, R. Singhal, F. Langa and G. D. Sharma, *Sol. RRL*, 2020, **4**, 2000460.

37 F. G. Guijarro, P. Malhotra, G. Gupta, R. Caballero, P. de la Cruz, R. Singhal, G. D. Sharma and F. Langa, *J. Mater. Chem. C*, 2020, **8**, 4763–4770.

38 C. Xu, Z. Zhao, K. Yang, L. Niu, X. Ma, Z. Zhou, X. Zhang and F. Zhang, *J. Mater. Chem. A*, 2022, **10**, 6291–6329.

39 M. Alonso-Abella, F. Chenlo, G. Nofuentes and M. Torres-Ramirez, *Energy*, 2014, **67**, 435–443.

40 R. Gottschalg, D. Infield and M. Kearney, *Sol. Energy Mater. Sol. Cells*, 2003, **79**, 527–537.

41 C. A. F. Ramos, A. N. Alcaso and A. J. M. Cardoso, *IOP Conf. Ser.: Earth Environ. Sci.*, 2019, **354**, 012048.

42 A. Luque and S. Hegedus, *Handbook of PV Science and Engineering*, Wiley, Chichester, 2003, pp. 905–967.

43 A. Landi and D. Padula, *J. Mater. Chem. A*, 2021, **9**, 24849–24856.

44 C. A. Tan and B. T. Wong, *Sol. RRL*, 2021, **5**, 2100503.

45 A. Landi, A. Landi, A. Velardo and A. Peluso, *ACS Appl. Energy Mater.*, 2022, **5**, 10815–10824.

46 L. Wang, G. Nan, X. Yang, Q. Peng, Q. Li and Z. Shuai, *Chem. Soc. Rev.*, 2010, **39**, 423–434.

47 A. Landi, A. Landi, A. Leo and A. Peluso, *J. Chem. Phys.*, 2024, **160**, 174114.

48 A. Landi, R. Borrelli, A. Capobianco, A. Velardo and A. Peluso, *J. Phys. Chem. C*, 2018, **122**, 25849–25857.
49 A. Landi, *J. Phys. Chem. C*, 2019, **123**, 18804–18812.
50 A. Velardo, R. Borrelli, A. Capobianco, A. Landi and A. Peluso, *J. Phys. Chem. C*, 2019, **123**, 14173–14179.
51 Y. Niu, Q. Peng, C. Deng, X. Gao and Z. Shuai, *J. Phys. Chem. A*, 2010, **114**, 7817–7831.
52 R. Kubo and Y. Toyozawa, *Prog. Theor. Phys.*, 1955, **13**, 160–182.
53 M. Lax, *J. Chem. Phys.*, 1952, **20**, 1752–1760.
54 R. Borrelli and A. Peluso, *Wiley Interdiscip. Rev.: Comput. Mol. Sci.*, 2013, **3**, 542–559.
55 A. Capobianco, R. Borrelli, A. Landi, A. Velardo and A. Peluso, *J. Phys. Chem. A*, 2016, **120**, 5581–5589.
56 G. Long, A. Li, R. Shi, Y.-C. Zhou, X. Yang, Y. Zuo, W.-R. Wu, U.-S. Jeng, Y. Wang, X. Wan, P. Shen, H.-L. Zhang, T. Yan and Y. Chen, *Adv. Electron. Mater.*, 2015, **1**, 1500217.
57 G. Zhang, X.-K. Chen, J. Xiao, P. C. Y. Chow, M. Ren, G. Kupgan, X. Jiao, C. C. S. Chan, X. Du, R. Xia, Z. Chen, J. Yuan, Y. Zhang, S. Zhang, Y. Liu, Y. Zou, H. Yan, K. S. Wong, V. Coropceanu, N. Li, C. J. Brabec, J.-L. Bredas, H.-L. Yip and Y. Cao, *Nat. Commun.*, 2020, **11**, 3943.
58 A. Troisi and G. Orlandi, *Chem. Phys. Lett.*, 2001, **344**, 509–518.
59 A. Landi and A. Troisi, *J. Phys. Chem. C*, 2018, **122**, 18336–18345.
60 T. Nematiaram, D. Padula, A. Landi and A. Troisi, *Adv. Funct. Mater.*, 2020, **30**, 2001906.
61 A. Muñoz-Losa, C. Curutchet, I. F. Galván and B. Mennucci, *J. Chem. Phys.*, 2008, **129**, 034104.
62 M. Di Donato, A. Iagatti, A. Lapini, P. Foggi, S. Cicchi, L. Lascialfari, S. Fedeli, S. Caprasecca and B. Mennucci, *J. Phys. Chem. C*, 2014, **118**, 23476–23486.
63 M. J. Frisch, G. W. Trucks, H. B. Schlegel, G. E. Scuseria, M. A. Robb, J. R. Cheeseman, G. Scalmani, V. Barone, G. A. Petersson, H. Nakatsuji, X. Li, M. Caricato, A. V. Marenich, J. Bloino, B. G. Janesko, R. Gomperts, B. Mennucci, H. P. Hratchian, J. V. Ortiz, A. F. Izmaylov, J. L. Sonnenberg, D. Williams-Young, F. Ding, F. Lipparini, F. Egidi, J. Goings, B. Peng, A. Petrone, T. Henderson, D. Ranasinghe, V. G. Zakrzewski, J. Gao, N. Rega, G. Zheng, W. Liang, M. Hada, M. Ehara, K. Toyota, R. Fukuda, J. Hasegawa, M. Ishida, T. Nakajima, Y. Honda, O. Kitao, H. Nakai, T. Vreven, K. Throssell, J. A. Montgomery, Jr., J. E. Peralta, F. Ogliaro, M. J. Bearpark, J. J. Heyd, E. N. Brothers, K. N. Kudin, V. N. Staroverov, T. A. Keith, R. Kobayashi, J. Normand, K. Raghavachari, A. P. Rendell, J. C. Burant, S. S. Iyengar, J. Tomasi, M. Cossi, J. M. Millam, M. Klene, C. Adamo, R. Cammi, J. W. Ochterski, R. L. Martin, K. Morokuma, O. Farkas, J. B. Foresman and D. J. Fox, *Gaussian 16 Revision C.01*, Gaussian Inc., Wallingford CT, 2016.
64 S. M. Falke, C. A. Rozzi, D. Brida, M. Maiuri, M. Amato, E. Sommer, A. De Sio, A. Rubio, G. Cerullo, E. Molinari and C. Lienau, *Science*, 2014, **344**, 1001–1005.
65 S. Giannini, A. Carof and J. Blumberger, *J. Phys. Chem. Lett.*, 2018, **9**, 3116–3123.
66 S. Fratini, S. Ciuchi, D. Mayou, G. T. De Laissardière and A. Troisi, *Nat. Mater.*, 2017, **16**, 998–1002.
67 D. Lee, H. Hwang, D. H. Sin, C. Park, S. G. Han, J. Mun, J. Noh, S. H. Kim, H. Kim, H. Lee, C. Lee, J. Rho, K. Cho and M. S. Jeong, *ACS Energy Lett.*, 2021, **6**, 2610–2618.
68 R. Wang, J. Xu, L. Fu, C. Zhang, Q. Li, J. Yao, X. Li, C. Sun, Z.-G. Zhang, X. Wang, Y. Li, J. Ma and M. Xiao, *J. Am. Chem. Soc.*, 2021, **143**, 4359–4366.
69 M. S. Kotova, G. Londi, J. Junker, S. Dietz, A. Privitera, K. Tvingstedt, D. Beljonne, A. Sperlich and V. Dyakonov, *Mater. Horiz.*, 2020, **7**, 1641–1649.
70 D. Padula, A. Landi and G. Prampolini, *Energy Adv.*, 2023, **2**, 1215–1224.
71 W. Li, Y. Yan, Y. Gong, J. Cai, F. Cai, R. S. Gurney, D. Liu, A. J. Pearson, D. G. Lidzey and T. Wang, *Adv. Funct. Mater.*, 2017, **28**, 1704212.

